JOURNAL OF CATALYSIS 142, 561–571 (1993)

Effect of Water Vapor on the Selective Reduction of NO by Methane over Cobalt-Exchanged ZSM-5

YUEJIN LI, PAULA J. BATTAVIO, AND JOHN N. ARMOR*

Air Products and Chemicals, Inc., 7201 Hamilton Boulevard, Allentown, Pennsylvania 18195

Received February 11, 1993; revised March 26, 1993

The effect of water vapor on the reduction of NO with CH_4 in excess O_2 over a Co–ZSM-5 catalyst was studied. The presence of 2% water significantly decreases the NO conversion at $T \leq 450$°C but has less of an effect at $T \geq 500$°C. The selectivity of methane toward NO reduction was enhanced by the presence of water at low temperatures and is unchanged at high temperatures. This inhibition is reversible upon eliminating water from the system. The effect of water is dependent on the level of water added, space velocity, reaction temperature, and level of methane in the feed. The addition of water increases the empirical reaction order with respect to either CH_4 or NO from a fractional order to first order. Temperature-programmed desorption studies show that the amount of NO adsorption on Co–ZSM-5 is significantly reduced if it is not fully dried, and the competitive adsorption between H_2O and NO is probably the cause of the inhibition by water. In addition, Co–ZSM-5 is capable of removing NO and CO simultaneously in either a dry or wet feed. © 1993 Academic Press, Inc.

INTRODUCTION

Technically, selective catalytic reduction of NO_x with methane in an oxidizing atmosphere is an attractive alternative to the currently practiced technology which uses ammonia as a reductant. Using methane as a selective reducing agent, one can eliminate the disadvantages associated with the SCR (selective reduction of NO_x with ammonia) technology, such as ammonia slip (breakthrough of unreacted ammonia), transportation of ammonia through residential areas, and equipment corrosion. Further, natural gas is readily available in most parts of the world and is widely used as a fuel source for many industrial utilities and engines.

Recently Li and Armor (*1, 2*) reported a family of metal exchanged zeolite catalysts which can effectively reduce NO_x with CH_4 in the presence of excess O_2. With a Co–ZSM-5 catalyst, NO was completely reduced to N_2 at 400°C. Unlike previous reports with metals and oxides (*3*), the presence of O_2 actually enhanced the NO conversion significantly on the Co–ZSM-5 catalyst. Co–ZSM-5 is not active for the direct NO decomposition—the presence of CH_4 and O_2 are necessary (*1*). The NO conversion is proportional to the level of CH_4 in the feed. The following two reactions are involved in this process, NO reduction by CH_4 (reaction (1)) and CH_4 combustion (reaction (2)):

$$2NO + CH_4 + O_2 \rightarrow N_2 + CO_2 + 2H_2O \quad (1)$$

$$CH_4 + 2O_2 \rightarrow CO_2 + 2H_2O. \quad (2)$$

This remarkable chemistry is attributed to the cobalt cations which are anchored by certain types of zeolites, e.g., ZSM-5. Cu–ZSM-5 is a unique catalyst for NO decomposition to its elements and a good catalyst for NO reduction with C_{2+} hydrocarbons, and it has been studied extensively by many groups over the past few years (*4–21*). However, Cu–ZSM-5 is ineffective for the NO reduction with CH_4, where CH_4 reacts with O_2 preferentially (reaction (2)) instead of with NO (reaction (1)). The very active extralattice oxygens in Cu–ZSM-5

* To whom correspondence should be addressed.

0021-9517/93 $5.00

may contribute to its low selectivity for the NO reduction. On the other hand, Mn- and Ni-exchanged ZSM-5 have similar, although slightly lower, activities/selectivities compared to Co–ZSM-5. In addition, the type of zeolite is also very important. Besides ZSM-5, mordenite is also a good support for cobalt for this reaction, but Co–Y is a poor catalyst, even though it has much higher cobalt loading. Cobalt oxides supported on conventional inorganic oxide supports are inactive for this reaction.

A very important question is what is the effect of H_2O upon reaction (1). There are two possible sources of water. Most flue gas streams which contain NO_x also contain large amounts of H_2O (2–18%), hence H_2O tolerance is an important issue regarding a useful catalyst. For all practical purposes, studies of de-NO_x catalysts should be carried out in the presence of water vapor. Further, by using CH_4, H_2O is also a product of the reaction. Therefore, it may influence the kinetics of the reaction.

SCR is the only commercially available catalytic technology to selectively remove NO_x from stationary streams. The H_2O effect on the SCR activity and selectivity over a vanadia supported on silica-titania catalyst was studied by Odenbrand *et al.* (*22*). They reported that the addition of 1% H_2O changed the NO conversion slightly, the direction of the change depended on reaction temperature. However, the presence of H_2O significantly suppressed the N_2O (a by-product of SCR) formation, increasing the selectivity toward N_2 formation. Similar observations were also reported by Topsøe *et al.* (*23*) on a vanadia–titania catalyst. Based on their TPD and IR experiments, they concluded that water adsorbed on the vanadia surface more weakly than ammonia and therefore did not inhibit the adsorption of ammonia under SCR conditions. It was suggested that the adsorption of ammonia could not be a rate-limiting step in the SCR reaction. The effects of H_2O on the activities of NO decomposition (*7, 9*) and reduction by C_{2+} hydrocarbons (*19–21*) was reported on Cu–ZSM-5. However, its effect on kinetics and the nature of the effect have not been reported in literature. In this paper, we discuss the effect of water vapor on the NO reduction by methane (on NO reduction activity, selectivity, and the kinetics) and the nature of the effect.

EXPERIMENTAL

Catalyst Preparation

The preparation of Co–ZSM-5 and other metal exchanged zeolite catalysts were described in detail elsewhere (*1, 2*). Briefly, Co–ZSM-5 was prepared by exchanging ~0.02 *M* Co^{2+} (acetate) into Na–ZSM-5 in an aqueous solution at 80°C for 24 h. The catalyst has the following composition: Si/Al = 13.6, Co/Al = 0.70 (4.0 wt% Co) and Na/Al = 0.0.

Reaction Studies

The catalytic activities were measured using a microcatalytic reactor in a steady-state plug flow mode. The reactor was a U-shaped glass tube with $\frac{1}{4}$″ o.d. at the inlet and $\frac{3}{8}$″ o.d. at the outlet. To reduce pressure drop, the catalyst was pelletized, crushed and then sieved to 60–80 mesh before use. Normally a 0.10-g sample was used for activity measurement. Kinetic studies, e.g., reaction order determinations, were made using a 0.05-g sample for reactions under dry conditions and 0.1 g under wet conditions, and NO conversions were controlled below 30%. The reaction mixture was obtained by blending four channels of flow, i.e., NO/He, CH_4/He, O_2/He, and He, and each was controlled by an independent mass flow controller. All gases were obtained from Air Products and Chemicals, Inc., as certified standards and used without further purification. The reaction mixture typically consisted of 820 ppm NO, 1015 ppm CH_4, and 2.5% O_2, and the total flow rate was 100 cc/min. (The typical GHSV was 30,000 based on the apparent bulk density of the zeolite catalyst, ~0.5 g/cm^3). A temperature programmer (Yokogawa, Model UP 40) with a J-type thermocouple in contact with the

catalyst bed was used to control the temperature. The catalyst was pretreated *in situ* in flowing He at 500°C for 1 h at a ramp rate of 5°C/min.

Water vapor was added to the feed using an H_2O saturator comprised of a sealed glass bubbler with a medium-pore frit immersed into deionized H_2O. Helium (25 cc/min) flowed through the bubbler, carrying the H_2O vapor to the feed. The bubbler was surrounded by a heating tape and insulated by glass wool. The temperature of the bubbler was controlled by a temperature controller. Different amounts of H_2O could be added to the feed by adjusting the bubbler temperature. To avoid any condensation of H_2O vapor, the gas line containing H_2O vapor was heat traced to a temperature higher than the saturation temperature. To protect the GC column from excessive H_2O, an ice-cooled H_2O condenser was incorporated downstream of the reactor but before GC sampling valve to condense out most of the H_2O vapor.

A Varian 6000 gas chromatograph with a TCD detector was used to monitor catalytic activity. A molecular sieve 5A column ($\frac{1}{8}$" × 10') was used to separate O_2, N_2 and CH_4 at 25°C. Occasionally, a Porapak Q column (column temperature = 50°C) was used to analyze for CO_2 formation and check the material balance. Near 100% carbon balance was achieved. [CH_4 was oxidized to CO_2.] An on-line mass spectrometer (UTI 100C) equipped with an on-line, atmospheric sampling device, was also used to monitor the gas effluent. Both the GC and MS could be operated simultaneously.

The NO conversion was calculated based on the N_2 formation (NO conversion = $2[N_2]/[NO]_0 \times 100\%$, where $[N_2]$ is the concentration of N_2 as a product and $[NO]_0$ is the inlet NO concentration.), and the CH_4 conversion based on the CH_4 consumption. (CH_4 conversion = $\{([CH_4]_0 - [CH_4])/[CH_4]_0\} \times 100\%$, where $[CH_4]_0$ is the inlet CH_4 concentration and $[CH_4]$ is the CH_4 concentration after reaction.) The selectivity index (α) is defined as the fraction of the reductant (CH_4) that is used up to reduce NO to N_2, i.e., the ratio of the consumption rate of CH_4 for reaction (1) (r_1) to the total consumption rate (r_t) of CH_4 (reactions (1) and (2)), and α can be calculated based upon Eq. (3),

$$\alpha = \frac{r_1}{r_t} = \frac{0.5 \times [NO]_0 \times C_{NO}}{[CH_4]_0 \times C_{CH_4}} \times 100\%, \quad (3)$$

where $r_1 = 0.5 \times F_t \times [NO]_0 \times C_{NO}$, F_t is the total flow rate, $[NO]_0$ is the inlet concentration of NO, and C_{NO} is the conversion of NO; $r_t = F_t \times [CH_4]_0 \times C_{CH_4}$, $[CH_4]_0$ is the inlet concentration of CH_4, and C_{CH_4} is CH_4 conversion. Consequently, $(1 - \alpha)$ is the fraction of CH_4 reacted with O_2. The reduction rate of NO (r_{NO}) [mmol/h-g] = $F_{NO} C_{NO}/W$, where, F_{NO} is the flow rate of NO [mmol NO/h] and W the weight of the catalyst [g]. Steady-state conversions at a temperature or feed composition were collected within a period of 1 to 2 h, and only stable data were used.

Temperature Programmed Desorption

For a typical TPD measurement, a 0.1-g sample was used, which is about 0.5 cm deep. The Co–ZSM-5 catalyst was pretreated to achieve different degrees of dehydration: (a) dried at 500°C for 1 h in flowing He (100cc/min.), (b) dried at 150°C for 1 h in flowing He, and (c) untreated (stored in the laboratory at 25°C for a long time.) The NO adsorption was carried out at 25°C by flowing a NO/He mixture (1640 ppm, 100 cc/min.) through the sample, and the effluent of the reactor was continuously monitored by a mass spectrometer (UTI 100C); the leveling-off in NO intensity indicated the saturation of the sample with NO. A color change (from light blue to light brown) was observed during the NO adsorption on a dry Co–zeolite sample, and this color change progressed down the bed as the adsorption proceeded. Typically, a period of 15 min was sufficient to achieve a saturation for NO adsorption. During NO adsorption, no other species was observed. After the NO adsorp-

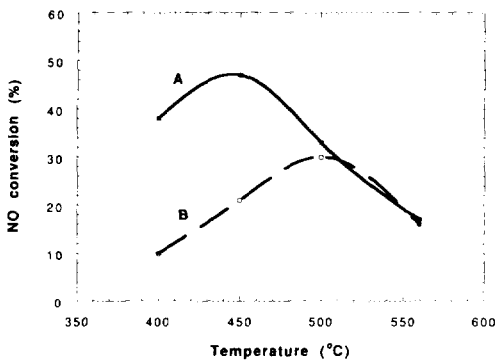

FIG. 1. Effect of water addition on the NO conversion over Co–ZSM-5 as a function of reaction temperature. The reaction was run at GHSV = 30,000, [NO] = 820 ppm, [CH_4] = 1015 ppm, and [O_2] = 2.5% ([H_2O] = 2% for the wet feed). The reaction was run first with the dry feed with increasing temperature (line A), then 2% water vapor was added at 560°C and the reaction was run with decreasing temperature (line B). Data were collected at each temperature for a period 1 to 2 h, and only stable, averaged data are shown.

tion, the sample was then flushed with a stream of He (100 cc/min) at 25°C to eliminate gaseous NO and weakly adsorbed NO. As the gaseous NO level, monitored by the mass spectrometer, returned to near the background level of the mass spectrometer, the sample was heated to 500°C at a ramp rate of 8°C/min in flowing He (100 cc/min.), and the desorbed species were monitored continuously by the mass spectrometer as a function of time/temperature. The mass spectrometer was calibrated for N_2, O_2, NO, N_2O, and other relevant species, and therefore quantitative analysis was possible. The amount of the NO adsorbed on catalyst was obtained by integrating the desorption rate vs time.

RESULTS AND DISCUSSION

The effect of H_2O vapor addition on the NO conversion over a Co–ZSM-5 catalyst is shown in Fig. 1 as a function of reaction temperature. Addition of 2% H_2O in the feed significantly reduces the NO conversion at low temperatures, ≤450°C, and the effect is small at high temperatures, ≥500°C. In both cases, NO conversion displays a volcano-shape curve with increasing temperature. With addition of 2% H_2O in the feed, the optimum NO conversion is shifted from 450 to 500°C. [At high temperatures the bending over of NO conversion is a more serious problem than the H_2O effect.] Like the temperature dependence, which is reversible on decreasing temperature (*1*), the effect of H_2O vapor is also entirely reversible (curve A was reproducible) upon drying the catalyst at 500°C for 1 h in a flow of He. This suggests that the H_2O effect is a kinetic phenomenon rather than due to structural damage of the catalyst. In fact, the NO conversion is stable for several days during continued operation with a wet feed at 500°C, and the XRD pattern of this spent Co–ZSM-5 catalyst is essentially identical to that of fresh one. This further illustrates that the catalyst structure is stable even under high-temperature, wet conditions.

Addition of H_2O vapor also suppresses the CH_4 conversion (Fig. 2); on the average the CH_4 conversion curve shifts 50°C higher upon addition of 2% H_2O. Thus, H_2O inhibits not only the NO reduction (Eq. (1)) but also the CH_4 combustion (Eq. (2)). It was suggested previously (2) that under dry conditions the decrease of NO conversion with increasing temperature was partially due to

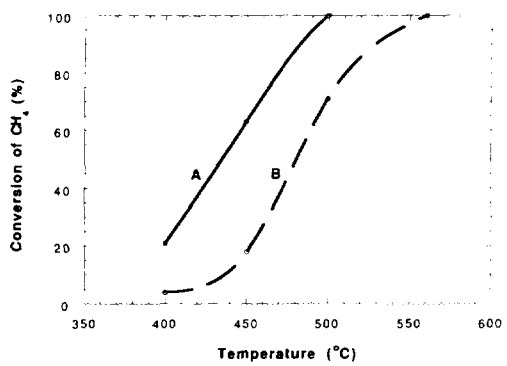

FIG. 2. Effect of water addition on the CH_4 conversion over Co–ZSM-5 as a function of reaction temperature. The data were collected based on the same experiment shown in Fig. 1 (line A, dry feed; line B, wet feed).

TABLE 1

Effect of H_2O Addition on CH_4 Selectivity Index[a] (%)

Temperature (°C)	GHSV = 30000		GHSV = 7500	
	Dry	Wet	Dry	Wet
400	75	97	50	61
450	30	52	25	28
500	13	18	15	15
560	7	6	—	—

[a] The reactions were run on a Co–ZSM-5 catalyst with [NO] = 820 ppm, [CH_4] = 1015 ppm, [O_2] = 2.5%, and [H_2O] = 2% (wet runs).

the depletion of CH_4 caused by its combustion (reaction (2)). The presence of H_2O suppresses the CH_4 conversion (Fig. 2), and therefore also shifts the temperature for the maximum in NO conversion from 450 to 500°C (Fig. 1). The effect of H_2O addition on CH_4 selectivity index is shown in Table 1 at two space velocities. In general, the presence of H_2O increases the selectivity index at low temperatures, e.g., from 75 to 97% at 400°C and GHSV = 30,000, while at high temperatures H_2O has little effect on the selectivity index. Further, with a low space velocity (more catalyst or lower flow rate), the effect of H_2O on CH_4 selectivity index is much less significant even at 400°C, i.e., 50 vs 61%.

Water is a product of the NO reduction, and ~0.1% H_2O could be generated from the reactions. Therefore, it is necessary to test the catalyst with H_2O levels ranging from a few tenths of a percent to a few percent (Fig. 3). With the addition of <0.2% H_2O, the NO conversion decreases sharply at 450°C. However, with a further increase of the level of H_2O, its impact on NO conversion is rather mild. Note, both the inlet NO concentration (820 ppm) and the CH_4 concentration (1015 ppm) are much lower than the level of H_2O.

As shown in Fig. 4, under certain conditions the effect of H_2O on the NO conversion is rather small. With the addition of 2% H_2O, >60% of NO conversion is obtained with a GHSV of 7500, [NO] = 200 ppm,

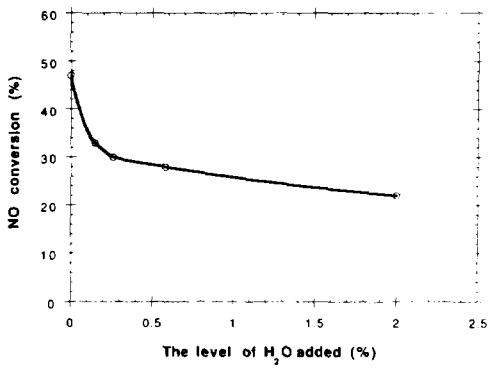

FIG. 3. The effect of water addition on the NO conversion over Co–ZSM-5 as a function of water level at 450°C. The reaction was run at GHSV = 30,000, [NO] = 820 ppm, [CH_4] = 1015 ppm, and [O_2] = 2.5%. The reaction was first run with a dry feed, by-passing the water saturator, then diverting a stream of He through the water saturator at different temperatures to achieve reported water levels.

[CH_4] = 1400 ppm, [CO] = 80 ppm, and at T = 400–450°C. It is obvious that the effect of H_2O over a Co–ZSM-5 catalyst is a function of space velocity and the level of CH_4 in the feed. The effect of water on the NO conversion can be partially compensated by increasing [CH_4] in the feed. Note, this feed also contains a very small amount of CO, 80 ppm. Our control run indicates that CO

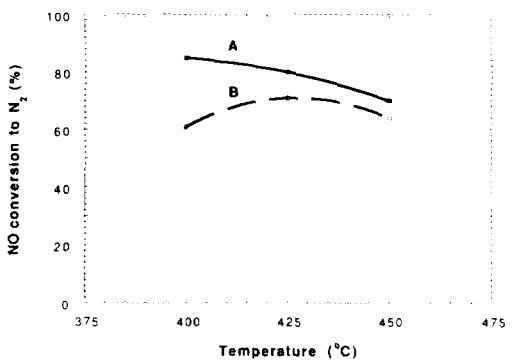

FIG. 4. Effect of water vapor on the NO conversion over Co–ZSM-5 at GHSV = 7500. The reaction was run with a feed consisting of 200 ppm NO, 1400 ppm CH_4, 2% O_2, and 80 ppm CO (2% water for wet feed) (line A, dry feed; line B, wet feed).

TABLE 2

Effect of H_2O on NO Conversions[a] (%) over Cation-Exchanged Zeolites

Catalyst	450°C		500°C	
	Dry	Wet[b]	Dry	Wet[b]
Co–ZSM-5	47	23	33	31
Co–mordenite	33	25	28	25
Mn–ZSM-5	31	23	39	36
Ni–ZSM-5	26	19	21	19
H–ZSM-5	16	~5	24	~2

[a] All reactions were run with a GHSV of 30,000, except on H–ZSM-5 (15,000 h^{-1}). The feed consisted of 820 ppm NO, 1015 ppm CH_4, and 2.5% O_2.
[b] $[H_2O]$ = 2%.

is ineffective as a selective reducing agent for NO in an oxidizing atmosphere. However, here CO is 100% oxidized to CO_2 under both dry and wet conditions. Therefore, Co–ZSM-5 is capable of removing both NO and CO simultaneously.

The addition of H_2O also suppresses the NO conversion on other metal-zeolite catalysts. As shown in Table 2, with a Co–mordenite catalyst (Si/Al = 5.3, Co/Al = 0.47), upon addition of 2% H_2O, the NO conversion decreases from 33 to 25% at 450°C, and 28 to 25% at 500°C. Over a Mn–ZSM-5, the NO conversion decreases from 31 to 23% and 39 to 36% at 450 and 500°C, respectively. H–ZSM-5, which has some activity for the NO reduction, is very sensitive to H_2O; with a GHSV of 15,000 (half of our typical space velocity), the NO conversion decreased from 16 to ~5% at 450°C and from 24 to ~2% at 500°C upon the addition of 2% H_2O in the feed.

A further examination of H_2O on the kinetics was made on the Co–ZSM-5 catalyst. Figures 5 and 6 show the influence of H_2O on rate of NO reduction as a function of the CH_4 and NO partial pressure, respectively. The presence of H_2O not only decreases the reaction rate significantly but also profoundly changes its empirical order with respect to both CH_4 and NO. Under dry conditions, fraction orders of 0.4–0.6 are repeatedly observed for both CH_4 and NO.

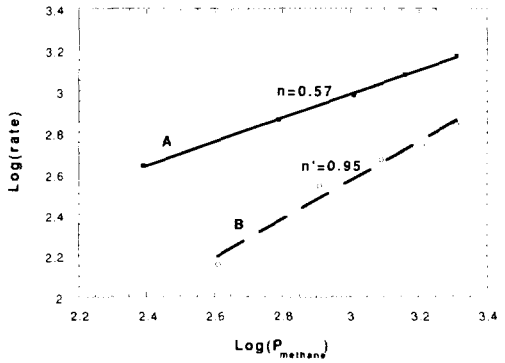

FIG. 5. Effect of water on the empirical reaction order with respect to CH_4 over Co–ZSM-5. Line A is a Log(rate) vs Log($P_{methane}$) plot under dry conditions ([NO] = 820 ppm, $[O_2]$ = 2.5%, T = 400°C, GHSV = 60,000); Line B is a Log(rate) vs Log($P_{methane}$) plot under wet conditions ($[H_2O]$ = 2%, [NO] = 820 ppm, $[O_2]$ = 2.5%, T = 450°C, and GHSV = 30,000). The NO reduction rate is defined in the Experimental section. The reaction orders are the slopes of the straight lines.

Interestingly, with the addition of 2% H_2O in the feed, the reaction orders are near 1.0 with respect to both CH_4 and NO.

To understand how H_2O affects the catalytic activity, temperature programmed desorption (TPD) experiments were made using a Co–ZSM-5 with different degrees of

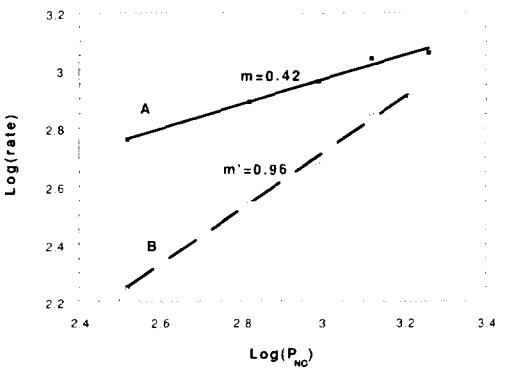

FIG. 6. Effect of water on the empirical reaction order with respect to NO over Co–ZSM-5. Line A is a Log(rate) vs Log(P_{NO}) plot under dry conditions ($[CH_4]$ = 820 ppm, $[O_2]$ = 2.5%, T = 400°C, and GHSV = 60,000); Line B is a Log(rate) vs Log(P_{NO}) plot under wet conditions ($[H_2O]$ = 2%, $[CH_4]$ = 1015 ppm, $[O_2]$ = 2.5%, T = 450°C, and GHSV = 30,000).

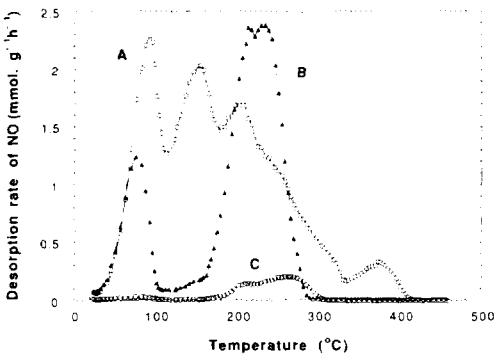

FIG. 7. TPD of NO on Co–ZSM-5 as a function of degree of dehydration. The sample was dried at 500°C in He flow for 1 h (A, —□—); at 150°C in He flow for 1 h (B, —▲—); and unpretreated (C, —O—) before NO adsorption at 25°C.

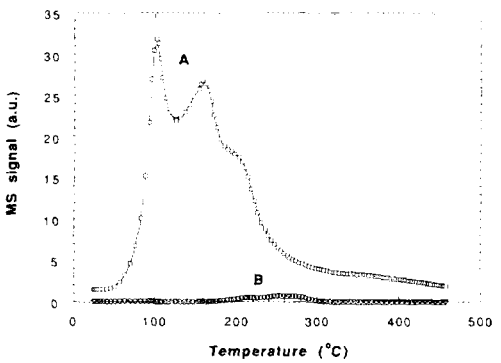

FIG. 8. TPD of NO (B) and H_2O (A) on an unpretreated Co–ZSM-5. The sample was flushed with He at 25°C before NO adsorption at the same temperature. The NO and H_2O signals were not calibrated.

dehydration. The NO TPD profiles are compared in Fig. 7. On the sample dried at 500°C, five NO desorption peaks were observed at ~90, 150, 210, 250, and 380°C, and the peak intensity decreased with increasing peak temperature. Quantitatively, the amount of NO adsorbed/desorbed is 0.74 mmol NO/g of catalyst. In contrast, the amount of NO adsorbed on the untreated sample (helium flushed at room temperature) is only 0.04 mmol/g, a factor of 19 smaller than that of the sample dried at 500°C. Although the total amount of NO adsorbed on the untreated sample is low, NO desorbed at rather high temperatures, and the low temperature desorption peaks are completely missing. The NO adsorption on this untreated sample at room temperature is very interesting. When a NO/He mixture is passed through the catalyst at 25°C, NO breakthrough was immediately observed followed by some displacement of H_2O by NO unlike on the fully dried Co–ZSM-5. Figure 8 illustrates the scale of the desorbed H_2O vs. NO on the untreated Co–ZSM-5.

On the partially dried Co–ZSM-5 (dried at 150°C for 1 h in flowing He), however, two peaks at 205 and 215°C were greatly enhanced (even higher than those of the fully dried catalyst), and the low-temperature peaks at 80°C are about one half of those with a dry catalyst (Fig. 7). Again, the desorption peak at 150°C was completely missing. The amount of NO adsorbed/desorbed is 0.45 mmol. NO/g (~60% of that on the dry catalyst). The TPD of H_2O and NO on this partially dried sample are shown in Fig. 9. An H_2O desorption peak was observed at ~190°C with a comparable intensity to the NO desorption peak followed by an very broad H_2O peak at 310°C with an extensive tailing beyond 450°C. This further shows the competitive nature of NO and H_2O adsorption. The similarity in shape be-

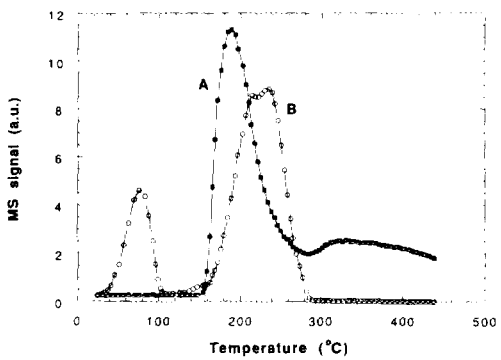

FIG. 9. TPD of NO (B) and H_2O (A) on a Co–ZSM-5 dried at 150°C in flowing He for 1 h. The NO was adsorbed on this sample at 25°C before the TPD measurement. The NO and H_2O signals were not calibrated.

tween the H_2O TPD and the NO TPD suggests that H_2O and NO may be adsorbed on the same sites.

The NO reduction by CH_4 generates H_2O as a product, and addition of H_2O significantly affects the reaction rate. Therefore, any meaningful reaction rate expression must include H_2O as a kinetic term. The significant decrease in NO reduction rate and dramatic change in empirical reaction order as the result of H_2O addition leads us to believe that the rate can be expressed in a Langmuir–Hinshelwood (LH) form,

$$\text{Reaction rate } (r) = \frac{k[\text{NO}][\text{CH}_4]}{1 + K_1[\text{NO}] + K_2[\text{H}_2\text{O}]} \quad (4)$$

where k is the apparent rate constant, K_1 is the NO adsorption equilibrium constant, and K_2 is H_2O adsorption equilibrium constant. [NO] and [H_2O] are concentrations of NO and H_2O, respectively. The rate expression (Eq. (4)) can then be rearranged, yielding

$$\frac{1}{r} = \frac{1}{k[\text{NO}][\text{CH}_4]} + \frac{K_1}{k[\text{CH}_4]} + \frac{K_2[\text{H}_2\text{O}]}{k[\text{NO}][\text{CH}_4]} \quad (5)$$

For the [NO] dependence studies (Fig. 6A, without the addition of H_2O), [CH_4] was held constant. Here, [H_2O] is the H_2O concentration generated from CH_4 oxidation. According to the reaction stoichiometry, one molecule CH_4 produces two H_2O molecules. Hence, [H_2O] = 2[CH4] × Conv. of CH_4. As shown in Fig. 10, the conversion of CH_4 is constant with varying [NO]. Therefore, [H_2O] is a constant. Thus, Eq. (5) can be simplified as

$$\frac{1}{r} = \alpha_0 + \frac{\alpha_1}{[\text{NO}]} \quad (6)$$

where $\alpha_0 = K_1/k[\text{CH}_4]$ and $\alpha_1 = (1 + K_2[\text{H}_2\text{O}])/k[\text{CH}_4]$. Inserting the data from Fig. 6A in Eq. (6) and plotting $1/r$ vs 1/[NO], we obtain a straight line, indicating that the proposed rate form is consistent with the data (see Fig. 11).

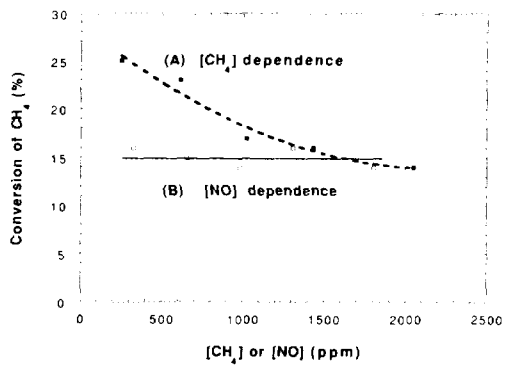

FIG. 10. Conversion of CH_4 as a function of CH_4 concentration (A) and NO concentration (B). These reactions were run at dry conditions at 400°C (line A, [NO] = 820 ppm, [O_2] = 2.5%, and GHSV = 60,000; line B, [CH_4] = 820 ppm, [O_2] = 2.5%, T= 400°C, and GHSV = 60,000).

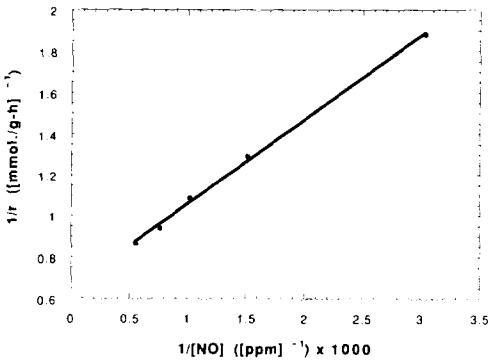

FIG. 11. A $1/r$ vs 1/[NO] plot. The data are derived from those shown in Fig. 6A.

For the [CH_4] dependence (Fig. 5A, no H_2O addition), [NO] was held constant and Eq. (5) can be written as

$$\frac{1}{r} = \frac{\beta_0 + \beta_1[\text{H}_2\text{O}]}{[\text{CH}_4]} \quad (7)$$

where, $\beta_0 = (1 + K_1[\text{NO}])/k[\text{NO}]$ and $\beta_1 = K_2/k[\text{NO}]$. However, here [$H_2O$] ([$H_2O$] = 2[$CH_4$ × Conv. CH_4) is not constant with changing [CH_4] (see Fig. 10). Equation (7) can be rearranged to

$$\frac{[\text{CH}_4]}{r} = \beta_0 + \beta_1[\text{H}_2\text{O}]. \quad (8)$$

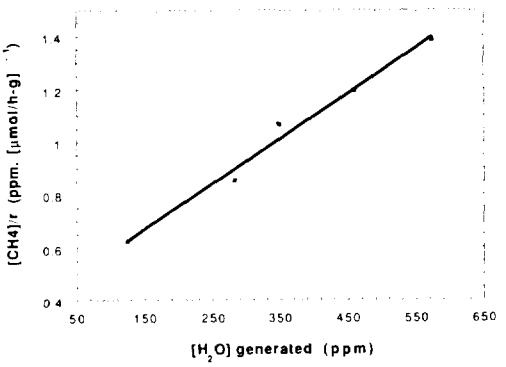

FIG. 12. A $[CH_4]/r$ vs $[H_2O]$ plot. The data are derived from those shown in Fig. 5A.

Again, plotting $[CH_4]/r$ vs $[H_2O]$, we obtain a straight line (Fig. 12). Therefore, our data are in agreement with the proposed rate expression.

Obviously, the fractional empirical reaction orders (Figs. 5 and 6) obtained under dry conditions reflect the inhibition terms in Eq. (4). On the other hand, with the addition of 2% H_2O [Note, the level of NO or CH_4 is on the order of 1000 ppm.], the value of denominator of Eq. (4) should be close to $K_2[H_2O]$ itself and is essentially constant. Consequently, we predict that

$$r = k'[NO][CH_4], \qquad (9)$$

which is what we observed.

The proposed rate expression Eq. (4) describes the NO reduction rate under our experimental conditions, i.e., in the presence of excess O_2. As we reported earlier (*1*), the NO reduction rate is proportional to $[O_2]$ at low O_2 levels, i.e., <0.5%, and independent of $[O_2]$ when $[O_2] > 0.5\%$. With excess O_2 in the feed, therefore, the O_2 term needs not appear in the rate equation.

In Eq. (4), NO and H_2O are the only adsorbed species. The possibility of CH_4 adsorption was also examined. Using a similar method to NO TPD, the adsorption of CH_4 on Co–ZSM-5 at room temperature could not be detected. Upon increasing temperature in a flow of CH_4/He mixture from 25 to 500°C, no appreciable CH_4 consumption was found, however, some CH_4 was decomposed as evidenced by the evolution of trace amount of H_2. Based on this experiment, we believe that the amount of CH_4 adsorbed on Co–ZSM-5 is not significant enough to alter the rate expression (Eq. (4)). On the other hand, the activation of (decomposition or adsorption of) CH_4 may be crucial in the reaction mechanism; CH_4 is likely involved in the formation of a reaction intermediate.

Metal exchanged zeolites are known to be oxygen carriers. In the case Cu–ZSM-5, an extralattice oxygen (ELO) atom can be held by two Cu^{2+} (*24*). The ELO can be released by reacting with CO or H_2 to form CO_2 and H_2O (*10*), consequently the Cu^{2+} is reduced to Cu^+. Cu^+ may be re-oxidized by exposing the zeolite to O_2 or NO. It is also widely recognized that the Cu–ZSM-5 may undergo self-reduction with the elimination of O_2. About 10% of the ELO can be released at 500°C in flowing He. This unique feature of Cu–ZSM-5 is regarded as a key requirement for sustained NO decomposition. There, the ELO is actively involved in the NO decomposition and is thought as the most abundant surface species (MASS).

Co–ZSM-5, however, has little activity for NO decomposition (*1*), and the Co–O bond is much stronger. Desorption of O_2 is never observed below 500°C. Even with CO flowing through a fully oxidized Co–ZSM-5 up to 500°C (*2*), ELO is still not released. Therefore, unlike on Cu–ZSM-5, it is very difficult to cycle through either Co^{2+}/Co^0, or Co^{3+}/Co^{2+} with the Co–ZSM-5 catalyst. This suggests that the redox property of Co–ZSM-5 is not important in the NO reduction by CH_4. Although there are abundant ELO atoms in Co–ZSM-5, their involvement in the NO reduction kinetics seems insignificant.

In light of above analysis, the surface NO coverage may be expressed as a Langmuir isotherm

$$\theta_{NO} = \frac{K_1[NO]}{1 + K_1[NO] + K_2[H_2O]}. \qquad (10)$$

The NO reduction rate then can be written as

$$r = k\theta_{NO}[CH_4]. \quad (11)$$

Our TPD data and the above kinetics analysis suggest that the inhibition effect of H_2O vapor on the NO reduction rate is the consequence of suppressed NO adsorption. It appears that at high temperatures the NO surface coverage is important, and therefore the adsorption of NO may be the rate determining step (RDS). At low temperatures, the NO coverage is relatively high. Thus, the RDS may be the activation of CH_4.

Practically speaking, the effect of H_2O is twofold, one being a kinetic phenomenon as discussed above and the other being its influence on physical structure of catalyst. The hydrothermal stability of a metal-exchanged zeolite catalyst depends not only the kind of zeolite but also the type of metal exchanged. The latter plays a very important role in stabilizing zeolite. Cu–ZSM-5 vs Co–ZSM-5 is a good example to illustrate this point. The effect of H_2O for the NO reduction by propane and propylene over a Cu–ZSM-5 catalyst was reported recently by several groups. Bartholomew *et al.* (*21*) found that on a Cu–ZSM-5 catalyst the NO conversion was significantly reduced by the presence of 14% H_2O between 300 and 600°C, e.g., from 61 to 19% at 400°C. After treatment with dry He at 300°C for 30 min, the NO conversion was not restored to its original level. This is not observed with Co–ZSM-5 using $NO/CH_4/O_2$.

Dramatic differences in hydrothermal stability between Cu–ZSM-5 and Co–ZSM-5 exist. Detailed catalyst deactivation by streaming was recently reported by Kharas *et al.* (*25*) who studied the deactivation of Cu–ZSM-5 under a typical automotive lean burn conditions (10% H_2O and GHSV = 127,000). They found that Cu–ZSM-5 was severely deactivated by exposing it to high temperature, wet exhaust gas. They reported significant pore volume loss for the deactivated Cu–ZSM-5, and this pore volume loss is not due to coke formation or dealumination of zeolite. Using EXAFS, they were able to detect a Cu–Cu coordination peak on the deactivated catalyst, while on their fresh Cu–ZSM-5 the only nearest neighbor of Cu is O atom. Comparing to Cu_2O and CuO, they concluded that the deactivation was primarily caused by metal sintering, and the zeolite structure change was only secondary. On the other hand, we did not see such hydrothermal instability for Co–ZSM-5. This may be the consequence of the difference in their redox properties; Cu in Cu–ZSM-5 is relatively easy to reduce to metal or oxidized to copper oxides, while a similar valence change for cobalt in Co–ZSM-5 is difficult. Alternatively, the hydrothermal stability of Co–ZSM-5 may be related to the degree of hydrolysis of cations in the zeolite.

CONCLUSIONS

Water vapor reduces the NO reduction activity by methane; this effect is more pronounced at low temperatures. However, at low temperatures, the addition of water vapor actually increases the CH_4 selectivity toward NO reduction. The water effect is proportional to the level of water added within a range of a few percent, and with a further increase of the water level the effect tends to be independent of the water. The effect of water is reversible upon eliminating water from the system, and the catalyst activity is stable under wet conditions. The presence of water also changes the empirical reaction order with respect to both NO and CH_4, with fractional orders under dry conditions and first order in NO and CH_4 under wet conditions. A kinetic model of Langmuir–Hinshelwood form was deduced to explain the kinetic data and the effect of water. Water competes with NO for adsorption sites, therefore, lowers the NO surface coverage. This competitive nature of water adsorption was further illustrated by the

TPD data collected on a Co–ZSM-5 at different degrees of dehydration; the amounts of NO adsorbed on partially dried and undried Co–ZSM-5 are significantly smaller than the fully dried sample. In contrast to Cu–ZSM-5, Co–ZSM-5 is much more stable in wet NO streams at high temperatures.

ACKNOWLEDGMENTS

Thanks are due to Tom Braymer for the catalyst preparation and to Frank Petrocelli and Harvey Stenger for first identifying the impact of water on the catalyst. We thank Air Products and Chemicals, Inc., for the permission to publish this work.

REFERENCES

1. Li, Y., and Armor, J. N., *Appl. Catal. B* **1,** L31 (1992).
2. Li, Y., and Armor, J. N., *Appl. Catal. B*, in press.
3. Adlhart, O. J., Hindin, S. G., and Kenson, R. E., *Chem. Eng. Prog.* **76,** 73 (1971).
4. Iwamoto, M., Furukawa, H., and Kagawa, S., *in* "New Developments in Zeolite Science and Technology" (Y. Mirikami, Ed.), p. 943. Elsevier, New York, 1989.
5. Iwamoto, M., Yahiro, H., and Tanda, K., *In* "Successful Design of Catalysts" (T. Inui Ed.), p. 19. Elsevier, Amsterdam, 1989.
6. Iwamoto, M., *in* "Future Opportunities in Catalytic and Separation Technologies" (M. Misono, Y. Moro-oka, and S. Kimura Eds.), p. 121. Elsevier, Amsterdam, 1990.
7. Iwamoto, M., Yahiro, H., Tands, K., Mizuno, N., Mine, Y., and Kagawa, S., *J. Phys. Chem.* **95,** 3727 (1991).
8. Iwamoto, M., Yohiro, H., Mizuno, N., Zhang, W.-X., Mine, Y., and Kagawa, S., *J. Phys. Chem.* **96,** 9360 (1992).
9. Li, Y., and Hall, W. K., *J. Phys. Chem.* **94,** 6145 (1990).
10. Li, Y., and Hall, W. K., *J. Catal.* **129,** 202 (1991).
11. Li, Y., and Armor, J. N., *Appl. Catal.* **76,** L1 (1991).
12. Hall, W. K., and Valyon, J., *Catal. Lett.* **15,** 311 (1992).
13. Valyon, J., and Hall, W. K., *in* "Proceedings, 10th International Congress on Catalysis, Budapest, 1992."
14. Spoto, G., Bordiga, S., Scarano, D., and Zecchina, A., *Catal. Lett.* **13,** 39 (1992).
15. Giamello, E., Murphy, D., Magnacca, G., Morterra, C., Shioya, Y., Nomura, T., and Anpo, M., *J. Catal.* **136,** 510 (1992).
16. Sarkany, J., d'Itri, J. L., and Sachtler, W. M. H., *Catal. Lett.* **16,** 241 (1992).
17. Sato, S., Yu-u, Y., Yahiro, H., Mizuno, N., and Iwamoto, M., *Appl. Catal.* **70,** L1 (1991).
18. Bennett, C. J., Bennett, P. S., Golunski, S. E., Hayes, J. W., and Walker, A. P., *Appl. Catal. A* **86,** L1 (1992).
19. Held, W., Konig, A., Richter, T., and Ruppe, L., SAE Paper No. 900496, 1990.
20. Iwamoto, M., and Mizuno, N., *J. Auto. Eng.*, **207,** 23 (1993).
21. Bartholomew, C. H., Gopalakrishnan, R., Stafford, P. R., Davison, J. E., and Hecker, W. C., AIChE 1992 Annual Meeting, Nov. 1–6, 1992, Miami Beach, FL, Paper 240a.
22. Odenbrand, C. U. I., Gabrielsson, P. L. T., Brandin, J. G. M., and Andersson, L. A. H., *Appl. Catal.* **78,** 109 (1991).
23. Topsøe, N. Y., Slaiak, T., Clausen, B. S., Srnak, T. Z., and Dumesic, J. A., *J. Catal.* **134,** 742 (1992).
24. Valyon, J., and Hall, W. K., submitted for publication.
25. Kharas, K. C. C., Robota, H. J., Liu, D. J., AIChE 1992 Annual Meeting, Nov. 1–6, 1992, Miami Beach, FL, Paper 240b.